Empirical Study of the Underwater Turbulence Effect on Non-Coherent Light

Citation for published version:
Geldard, CT, Thompson, J & Popoola, WO 2020, 'Empirical Study of the Underwater Turbulence Effect on Non-Coherent Light', *IEEE Photonics Technology Letters*, vol. 32, no. 20, 9180345, pp. 1307-1310. https://doi.org/10.1109/LPT.2020.3020368

Digital Object Identifier (DOI):
10.1109/LPT.2020.3020368

Link:
Link to publication record in Edinburgh Research Explorer

Document Version:
Peer reviewed version

Published In:
IEEE Photonics Technology Letters

Empirical Study of the Underwater Turbulence Effect on Non-Coherent Light

Callum T. Geldard, John Thompson, *Fellow, IEEE* and Wasiu O. Popoola, *Senior Member, IEEE*

***Abstract*—This letter presents an experimental study comparing the relative impact of turbulence induced scattering on coherent and non-coherent light propagating through water. It is shown that the scintillation index increases with increasing temperature inhomogeneity in the underwater channel. Our results indicate that a light beam from a non-coherent source has a greater resilience to temperature inhomogeneity induced turbulence effect in an underwater channel. These results will help researchers in simulating realistic channel conditions when modelling a light emitting diode (LED) based underwater optical wireless communication (UOWC) link.**

I. Introduction

Underwater optical wireless communications (UOWC) systems have to contend with the inherent optical properties (IOP) of water. These IOP are defined in terms of absorption and scattering of still water [1]. An important additional effect is turbulence, that can be understood as a case of random scattering. It is caused by fluctuations in the temperature and salinity yielding changes in refractive index along the channel [2].

The impact of turbulence induced scattering on a received signal can be quantified in terms of the scintillation index, σ_I^2, defined as [3]:

$$\sigma_I^2 = \frac{\langle I^2 \rangle - \langle I \rangle^2}{\langle I \rangle^2}, \tag{1}$$

where I is the received intensity and $\langle . \rangle$ denotes the ensemble average. References [4] and [5] have presented analytical expressions for σ_I^2 for laser and light emitting diode (LED) sources respectively. When modelling a turbulent channel through simulation, it is common to apply a fading coefficient to the channel gain, as in references [6]–[10]. Where [8], [9] simulate an LED as a monochromatic wide beam light source, and use $\sigma_I^2 > 0.1$ to calculate the fading coefficient.

Light emitted from a laser is coherent in both time and space. Temporal coherence means it has a small spectral width and can therefore be considered monochromatic. Spatial coherence, on the other hand, provides the property of directionality that allows for a narrow collimated beam. These properties are due to the structure of a laser and are not true for light emitted from an LED. As such the propagation of non-coherent light emitted by an LED is different to that of coherent light. Thus, it may not be accurate to simply use channel models developed for coherent propagation to model a non-coherent system. It can be noted that the analytical expressions for σ_I^2 with an LED given in reference [5] relate to monochromatic light.

Due to the lower cost and eye-safe properties, non-coherent LEDs are more suitable than the coherent laser in various applications. It is therefore vital that an understanding of the effect of turbulence on non-coherent light is developed.

The authors are with the School of Engineering, Institute for Digital Communications, Li-Fi Research and Development Centre, The University of Edinburgh, Edinburgh EH9 3JL, U.K. (e-mail: callum.geldard@sms.ed.ac.uk; j.s.thompson@ed.ac.uk; w.popoola@ed.ac.uk).

II. Related Works and Contribution

Whilst the effect of turbulence on coherent light has been experimentally evaluated in literature, including references [2], [11], [12], its effect on non-coherent light is less well understood. Some experimental measurement techniques, such as those described in references [13], [14], use a camera to measure the power spectrum of light transmitted from an LED array after propagating through a turbulent channel. In these related works, the refractive index structure constant of the underwater turbulence is estimated from wavefront measurements and the images of an array of LEDs. These earlier studies do not present a comparison of both coherent and non-coherent light sources in turbulent waters.

The key contribution of this paper is to present such a comparison based on experimental results. Turbulence from coherent and non-coherent light sources is estimated from the received signal intensity for both types of sources. Based on the measurements, we draw meaningful conclusions on the relative impact of temperature inhomogeneity induced underwater turbulence. These results will help researchers to accurately model LED based UOWC systems in turbulent water conditions and estimate a link margin based on these. We also aim to address the perpetuation of misinformation in literature that turbulence impacts laser and LED systems in the same way, as in references [8]–[10].

III. Experimental Methodology

A block diagram of the experimental set up is pictured in Fig. 1, showing the system level parts of the transmitter (Tx) and receiver (Rx), as well as the underwater channel emulator developed for this study. The channel emulator consists of a water tank of dimension $1.5 \times 0.5 \times 0.5$ m^3, filled with 225 litres of tap water in which underwater turbulence can be controlled. A square wave of peak-to-peak voltage (V_{pp}) 0.5 V is generated at 5 MHz for the Osram PL450b laser diode and 1 MHz for the Osram LD CN5M LED using a Keysight m8195a arbitrary waveform generator (AWG). A lower frequency is used to account for the bandwidth limitation of the LED. For both sources, a direct current (DC) bias of 40 mA is applied using a bias-T and the resultant biased signal

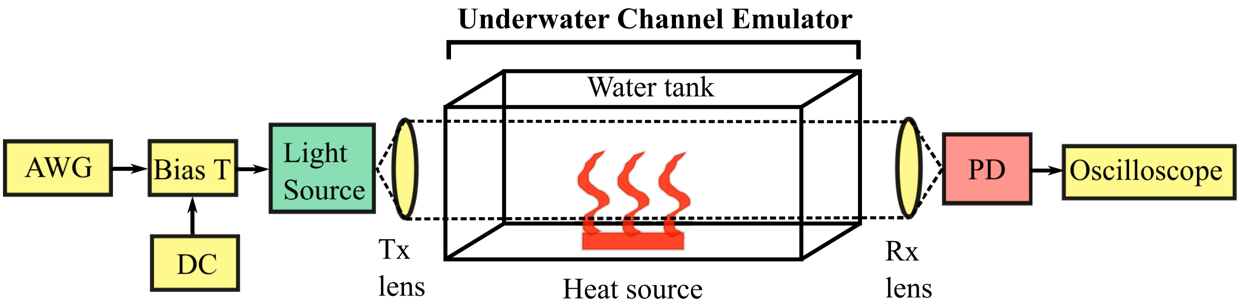

Fig. 1: Figure showing the system block diagram of the experimental set up used for the experiment.

is transmitted by either the laser or LED. This optical signal is then collimated using the Tx lens and transmitted through the underwater channel emulator. After propagating through the water tank the light beam is focused onto a photodiode (PD) using an optional Rx lens, chosen based on the beam width at the Rx. Photons are then captured by the PD contained in a New Focus 1601 photo-receiver and data points saved by an Agilent DSA8015 oscilloscope. The received V_{pp} is then recorded for 1000 iterations and the mean and variance calculated.

Underwater turbulence is created by generating a temperature inhomogeneity within the emulator. The temperature in the centre of the water tank is controlled using an aquarium heater. When heat is applied, it emanates a thin layer of hot water compared to the rest of the tank. This boundary between the different water temperatures induces turbulence in the channel. As the layer is thin, the orientation of the heating element relative to the light beam can be used to create multiple or single turbulence induced scattering. If it is parallel to the beam then photons are travelling along the layer boundary so they can be scattered multiple times as the shape and position of the boundary fluctuates. Conversely, when the heater is perpendicular to the beam, photons propagating undergo the lensing effect only once. These observations mean that although the transmission length is fixed throughout the experiment, the amount of turbulence induced scattering per link can be altered. The temperature is measured at four points within the emulator, two in the centre by the heat source and one each by the Tx and Rx respectively. The temperature difference within the channel emulator, ΔT, is the difference between the average of the temperature readings from the centre and the two outer thermometers.

Due to the spatial coherence of the laser source, the transmitted light can be collimated easily into a very narrow beam, while the LED cannot. Although this is a property of a coherent source, narrow beamwidths are not exclusive to lasers and the impact of beam diameter on σ_I^2 is known [4], [5]. Due to this, in order to confirm that the beamwidth is not the only factor contributing to any differences in σ_I^2, the laser is used with two different Tx lens configurations to produce collimated beams of different diameters. One has a diameter of approximately 4 mm and produces a narrow beam that remains collimated through the length of the channel. The other lens, the same as that used for the LED, is 4.5 cm in diameter and produces a wider collimated beam. They are referred to as narrow beam laser and the wide beam laser respectively hereafter.

IV. Experimental Results and Discussion

A. Scintillation Index and Temperature Difference

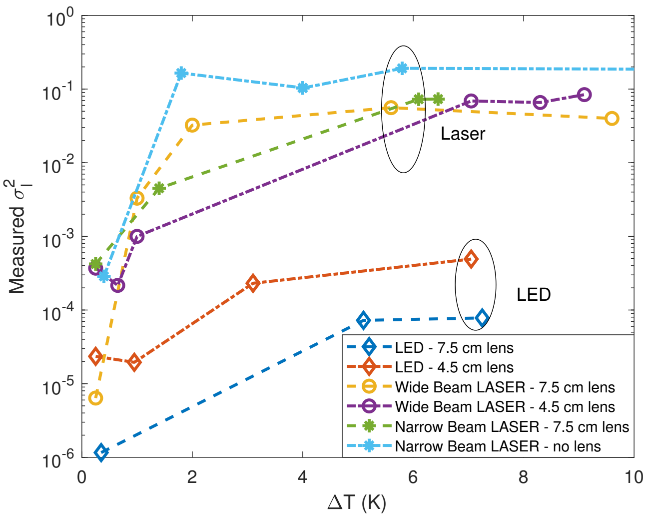

Fig. 2: Figure showing σ_I^2 vs ΔT for LED, wide beam laser, and narrow beam laser in clear water with multiple turbulence induced scattering boundary.

In this section we present our results and offer an explanation for the key findings. Following the experimental methodology previously described, the measured σ_I^2 could be found via (1). These are shown in Fig. 2 and 3 plotted against the observed ΔT in Kelvin (K). The overall trend across all channel conditions is that as ΔT increases, so too does the measured σ_I^2. There are, however, some fluctuations in this trend that can be ascribed to the random nature of the channel and the heating element. All results shown have $\sigma_I^2 < 1$ and are therefore in the weak turbulence regime.

Comparing the different light sources, it can be observed that the measured σ_I^2 is lower for the LED source than the collimated laser point source for all temperature gradients. In fact, the maximum σ_I^2 for any LED configuration is approximately 100 times lower for the multiple scattering in Fig. 2 and 10^4 times lower for the single scattering shown in

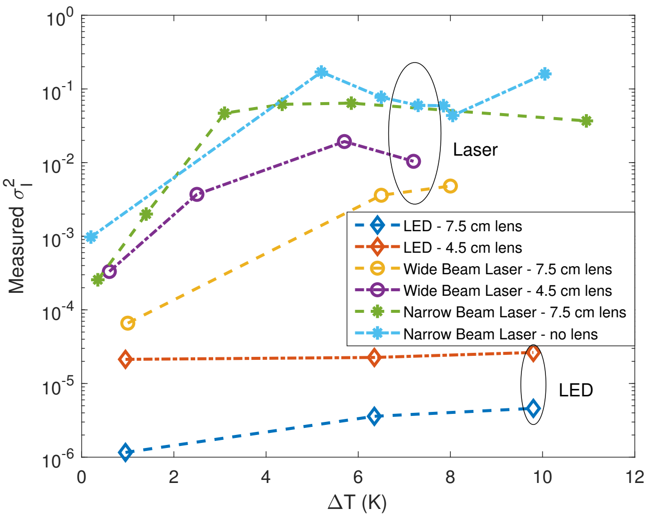

Fig. 3: Figure showing σ_I^2 vs ΔT for LED, wide beam laser, and narrow beam laser in clear water with a single turbulence induced scattering boundary.

Fig. 3. There are a number of explanations for this observation and they will be covered in the following discussion.

One possible explanation for the lower measured σ_I^2 for the LED compared to the laser is the aperture averaging effect when a larger Rx lens is used [12]. In order to discount this explanation from the study, the 7.5 cm Rx lens is used in combination with all three light sources as well as a smaller Rx lens for comparison. Here, the smaller lens is chosen to be similar to the beam diameter at the Rx in order to maximise the impact of turbulence. This can be seen in Fig. 2 and 3 by comparing the differences in σ_I^2 for the larger and smaller Rx lenses for each Tx configuration. The effect is greatest for the LED where it lowers σ_I^2 by approximately a factor of 10, although the benefit of using a larger Rx lens decreases when considering the laser beam. The results presented for LED and laser sources with Rx lenses of a similar size to the beam shows that the aperture averaging effect is not the reason for the reported differences in σ_I^2.

The impact of the beamwidth on σ_I^2 can be seen by comparing between the wide and narrow beam laser in each configuration. The difference is most clear in Fig. 3 for the case of a single turbulence induced scattering event where, for the 7.5 cm Rx lens, $\sigma_I^2 = 0.064$ when $\Delta T = 5.9$ K for the narrow beam laser but only 0.0036 for $\Delta T = 6.5$ K with the wide beam laser. However, for the case of multiple turbulence induced scattering events, as in Fig. 2, there is no such clear difference. Across both Fig. 2 and 3 the σ_I^2 value for both sizes of laser beam are orders of magnitude higher than that of the LED when a temperature inhomogeneity is applied to the channel. This implies that, although the beam diameter has an effect on σ_I^2, it is not the only reason for the reported differences as coherent and non-coherent beams with similar diameters yield very different results.

The results reported here can be explained in terms of beam width and coherence. A narrow beam laser can be understood as a point source, as such the whole beam is affected in the same way when it interacts with the turbulent layer. Wider beams, on the other hand, can be considered a disc source so different points within the beam footprint interact with different parts of the turbulent layer, so whilst one part of the beam may be scattered away from the Rx, another can be scattered towards it. Similarly, when light interacts with a turbulent layer, the change in propagation angle is dependent upon, among other things, its wavelength. This means that photons of different wavelengths are scattered in different directions upon interaction with the applied temperature inhomogeneity. The central wavelengths of the laser and LED are 450 nm and 452 nm respectively, implying that the dominant wavelength of each source will be affected similarly upon interaction with the temperature inhomogeneity. However, this wavelength dependency has implications on the value of σ_I^2 as, due to the temporal coherence of a laser source, the PL450b laser has a reported full width at half maximum (FWHM) of 2 nm, whereas the spectral width of the non-coherent LD CN5M LED is 25 nm. Resultantly light from a laser, with a narrow spectral bandwidth, is likely to all be scattered in the same manner. However, due to light from an LED consisting of a larger number of different wavelengths then there is a greater variation in scattering angles when it interacts with a turbulent layer. As such, the fluctuations in propagation path are different for each wavelength meaning some are scattered away whilst others are scattered towards the Rx, thus providing a form of wavelength diversity to mitigate the effects of turbulence.

B. Received Signal Distribution

Fig. 4 shows the histograms for some selected channel conditions from Fig 2. Histograms generated from the LED with 7.5 cm Rx lens and narrow beam laser with no Rx lens are chosen to highlight the differences between the signal received from coherent and non-coherent light sources with similar channel conditions. They are fitted with Gaussian and Log-Normal distributions, as well as the generalised gamma distribution (GGD) proposed for underwater turbulence in [11]. The related fit parameters and R^2 fit metric are presented in Table I. When $\sigma_I^2 \to 0$, all of these distributions converge to a Gaussian shape, as in Fig. 4a-4b. But as, σ_I^2 increases the Log-Normal and GGD distribution shapes are no longer Gaussian, as in Fig. 4c, when this happens the GGD provides the best fit for the channel conditions examined. Comparing these distribution shapes for LED and laser for similar ΔT values (5.1 and 5.8 K respectively) provides further evidence that non-coherent light has a greater resilience to underwater turbulence due to the fact that it is still Gaussian in shape whilst the distribution from the coherent source is distinctly non-Gaussian.

V. Conclusion

Through the measured experimental data presented in this letter, turbulence induced scattering is shown to have a greater impact on the propagation of coherent light, than for non-coherent light. This has implications for both system design

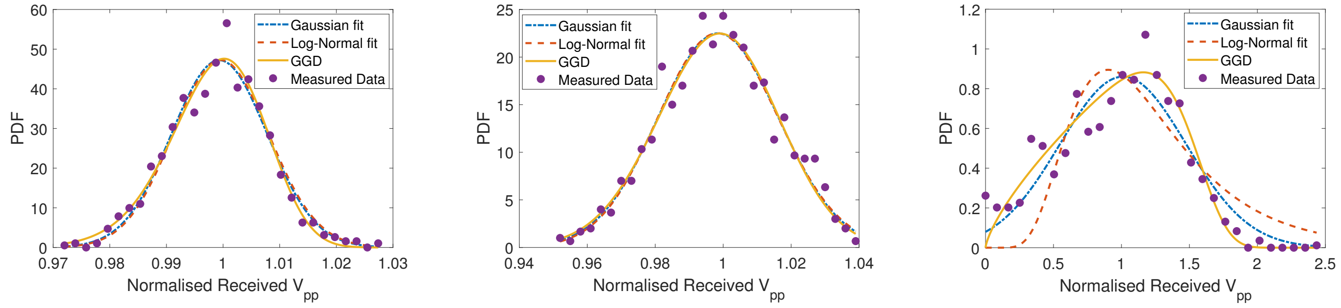

(a) LED, $\Delta T = 5.1$ K (b) Laser, $\Delta T = 0.4$ K (c) Laser, $\Delta T = 5.8$ K

Fig. 4: Figure showing recorded data from LED and narrow beam laser with similar channel conditions plotted as a histogram with Gaussian, Log-Normal, and GGD fits applied. The fitting parameters including σ_I^2 are displayed in Table I.

TABLE I: Fit parameters for Fig 4.

Fit	σ_I^2	Other parameters	R^2
LED, $\Delta T = 5.1$ K, measured $\sigma_I^2 = 7.24 \times 10^{-5}$			
Gaussian	7.14×10^{-5}	$m = 1.00$	0.97
Log-Normal	7.13×10^{-5}	$\mu = -3.60 \times 10^{-4}$	0.96
GGD	7.24×10^{-5}	$a = 5.70, b = 0.97, c = 50$	0.97
Laser, $\Delta T = 0.4$ K, measured $\sigma_I^2 = 2.87 \times 10^{-4}$			
Gaussian	3.14×10^{-4}	$m = 1.00$	0.96
Log-Normal	3.15×10^{-4}	$\mu = -1.40 \times 10^{-3}$	0.96
GGD	3.17×10^{-4}	$a = 40, b = 0.66, c = 8.9$	0.96
Laser, $\Delta T = 5.8$ K, measured $\sigma_I^2 = 0.1912$			
Gaussian	0.215	$m = 1.01$	0.87
Log-Normal	0.218	$\mu = 0.09$	0.66
GGD	0.175	$a = 0.22, b = 1.6, c = 7.8$	0.91

m mean of received signal intensity

μ log of the mean

a, b, c fitting parameters of GGD

R^2 Coefficient of determination

and simulation. Over the link distances achievable via LED based UOWC, it means turbulence can be omitted from link budget, thus simplifying design and reducing complexity. Similarly researchers simulating an LED based system can look to other, as yet unexplored, aspects of the channel rather than using unrealistically high values of σ_I^2. In a practical application, for a UOWC system over a short link in turbulent waters, it could be advantageous to use a low cost LED rather than a laser provided it meets the data rate requirements.

References

[1] C. D. Mobley. [Online]. Available: http://www.oceanopticsbook.info/

[2] D. J. Bogucki, J. A. Domaradzki, R. E. Ecke, and C. R. Truman, "Light scattering on oceanic turbulence," *Applied optics*, vol. 43, no. 30, pp. 5662–5668, 2004.

[3] H. Kaushal and G. Kaddoum, "Underwater optical wireless communication," *IEEE Access*, vol. 4, pp. 1518–1547, 2016.

[4] O. Korotkova, N. Farwell, and E. Shchepakina, "Light scintillation in oceanic turbulence," *Waves in Random and Complex Media*, vol. 22, no. 2, pp. 260–266, 2012. [Online]. Available: https://doi.org/10.1080/17455030.2012.656731

[5] Y. Baykal, "Scintillations of led sources in oceanic turbulence," *Appl. Opt.*, vol. 55, no. 31, pp. 8860–8863, Nov 2016. [Online]. Available: http://ao.osa.org/abstract.cfm?URI=ao-55-31-8860

[6] H. Jiang, H. Qiu, N. He, W. O. Popoola, Z. U. Ahmad, and S. Rajbhandari, "Performance of spatial diversity dco-ofdm in a weak turbulence underwater visible light communication channel," *Journal of Lightwave Technology*, pp. 1–1, 2020.

[7] J. Liu and Y. Dong, "On capacity of underwater optical wireless links under weak oceanic turbulence," in *OCEANS 2016 - Shanghai*, April 2016, pp. 1–4.

[8] M. Sharifzadeh and M. Ahmadirad, "Performance analysis of underwater wireless optical communication systems over a wide range of optical turbulence," *Optics Communications*, vol. 427, pp. 609 – 616, 2018. [Online]. Available: http://www.sciencedirect.com/science/article/pii/S0030401818306217

[9] F. Akhoundi, M. V. Jamali, N. B. Hassan, H. Beyranvand, A. Minoofar, and J. A. Salehi, "Cellular underwater wireless optical cdma network: Potentials and challenges," *IEEE Access*, vol. 4, pp. 4254–4268, 2016.

[10] W. Liu, Z. Xu, and L. Yang, "Simo detection schemes for underwater optical wireless communication under turbulence," *Photon. Res.*, vol. 3, no. 3, pp. 48–53, Jun 2015. [Online]. Available: http://www.osapublishing.org/prj/abstract.cfm?URI=prj-3-3-48

[11] H. M. Oubei, E. Zedini, R. T. ElAfandy, A. Kammoun, M. Abdallah, T. K. Ng, M. Hamdi, M.-S. Alouini, and B. S. Ooi, "Simple statistical channel model for weak temperature-induced turbulence in underwater wireless optical communication systems," *Opt. Lett.*, vol. 42, no. 13, pp. 2455–2458, Jul 2017. [Online]. Available: http://ol.osa.org/abstract.cfm?URI=ol-42-13-2455

[12] M. Yousefi, F. D. Kashani, A. Aghajani, and M. R. H. Rad, "Experimental study of the effects of thermally induced optical turbulence on underwater wireless optical communication link parameters," *Journal of Optics*, vol. 22, no. 2, p. 025702, 2020.

[13] A. V. Kanaev, S. Gladysz, R. A. de S Barros, S. Matt, G. A. Nootz, D. B. Josset, and W. Hou, "Measurements of optical underwater turbulence under controlled conditions," in *Ocean Sensing and Monitoring VIII*, W. W. Hou and R. A. Arnone, Eds., vol. 9827, International Society for Optics and Photonics. SPIE, 2016, pp. 28 – 35. [Online]. Available: https://doi.org/10.1117/12.2230256

[14] S. Gladysz, R. Barros, A. V. Kanaev, and W. Hou, "Characterization of underwater optical turbulence on the example of the Rayleigh-Benard water tank," in *Optics in Atmospheric Propagation and Adaptive Systems XX*, K. U. Stein and S. Gladysz, Eds., vol. 10425, International Society for Optics and Photonics. SPIE, 2017, pp. 57 – 65. [Online]. Available: https://doi.org/10.1117/12.2277539